PTEP

Prog. Theor. Exp. Phys. **2015**, 073B04 (21 pages)
DOI: 10.1093/ptep/ptv093

Criticality and inflation of the gauged $B - L$ model

Kiyoharu Kawana*

Department of Physics, Kyoto University, Kyoto 606-8502, Japan
*E-mail: kiyokawa@gauge.scphys.kyoto-u.ac.jp

Received April 28, 2015; Revised June 2, 2015; Accepted June 3, 2015; Published July 15, 2015

We consider the multiple point principle (MPP) and the inflation of the gauged $B - L$ (baryon number minus lepton number) extension of the Standard Model (SM) with a classical conformality. We examine whether the scalar couplings and their beta functions can become simultaneously zero at $\Lambda_{\rm MPP} := 10^{17}$ GeV by using two-loop renormalization group equations (RGEs). We find that we can actually realize such a situation and that the parameters of the model are uniquely determined by the MPP. However, as discussed by S. Iso and Y. Orikasa [Prog. Theor. Exp. Phys. **2013**, 023B08 (2013) [arXiv:1210.2848 [hep-ph]]], if we want to realize electroweak symmetry breaking by radiative $B - L$ symmetry breaking, the self-coupling λ_Ψ of a newly introduced SM singlet complex scalar Ψ must have a non-zero value at $\Lambda_{\rm MPP}$, which means the breaking of the MPP. We find that $\mathcal{O}(100)$ GeV electroweak symmetry breaking can be achieved even if this breaking is very small; $\lambda_\Psi(\Lambda_{\rm MPP}) \leq 10^{-10}$. Within this situation, the mass of the $B - L$ gauge boson is predicted to be $M_{B-L} = 2\sqrt{2} \times \sqrt{\lambda(v_h)/0.10} \times v_h \simeq 696\,\text{GeV}$, where λ is the Higgs self-coupling and v_h is the Higgs expectation value. This is a remarkable prediction of the (slightly broken) MPP. Furthermore, such a small λ_Ψ opens a new possibility: Ψ plays the role of the inflaton [28]. Another purpose of this paper is to investigate the $\lambda_\Psi \Psi^4$ inflation scenario with non-minimal gravitational coupling $\xi \Psi^2 \mathcal{R}$ based on two-loop RGEs.

Subject Index B02, B32, B40

1. Introduction

The discovery of the Higgs-like particle and its mass [1,2] is very meaningful for the Standard Model (SM). The experimental value of the Higgs mass suggests that the Higgs potential can be stable up to the Planck scale $M_{\rm pl}$ and also that both the Higgs self-coupling λ and its beta function β_λ become very small around $M_{\rm pl}$. This fact attracts much attention, and there are many works which try to find its physical meaning [3–22].

Well before the discovery of the Higgs, it was argued that the Higgs mass could be predicted to be around 130 GeV by the requirement that the minimum of the Higgs potential becomes zero at $M_{\rm pl}$ [3,4]. Such a requirement (not always at $M_{\rm pl}$) is generally called the multiple point principle (MPP). One of the good points of the MPP is its predictability: the low-energy effective couplings are fixed so that the minimum of the potential vanishes; see, e.g., Refs. [23,24].

By taking the fact that the MPP can be realized in the SM into consideration, a natural question is whether such a criticality can also be realized in the models beyond the SM. One interesting extension is the gauged $B - L$ (baryon number minus lepton number) model with a classical conformality [25–28]. Here, "classical conformality" means there is no mass term at the classical level without gravity. This model can be obtained by gauging the global $\mathrm{U}(1)_{B-L}$ symmetry of the SM with three right-handed neutrinos and an SM singlet complex scalar Ψ. As discussed in the following, if we

Funded by SCOAP[3]

neglect the Yukawa couplings between the Higgs and neutrinos, there are six unknown parameters in this model. In particular, two of them are new scalar couplings: κ and λ_Ψ. Therefore, in principle, these six parameters can be uniquely fixed by the MPP conditions:

$$\lambda(\Lambda_{\rm MPP}) = \lambda_\Psi(\Lambda_{\rm MPP}) = \kappa(\Lambda_{\rm MPP}) = \beta_\lambda(\Lambda_{\rm MPP}) = \beta_{\lambda_\Psi}(\Lambda_{\rm MPP}) = \beta_\kappa(\Lambda_{\rm MPP}) = 0, \tag{1}$$

where $\Lambda_{\rm MPP}$ is the scale at which we impose the MPP. The analyses in this paper are based on the following assumptions:

1. We consider the MPP at $\Lambda_{\rm MPP} = 10^{17}$ GeV.
2. As well as the analyses in Refs. [25,26], we do not include mass terms in the Lagrangian. As a result, all the low-energy scales are radiatively generated.
3. The Higgs mass is fixed at
$$M_h = 125.7\,{\rm GeV}, \tag{2}$$
and we regard the top mass M_t as one of the free parameters.
4. We assume that small neutrino masses are produced by the seesaw mechanism via radiative breaking of the $B-L$ symmetry. As a result, we can neglect the Yukawa couplings y_ν between the Higgs and neutrinos because the typical breaking scale is very small $(\ll 10^{13}\,{\rm GeV})$.

In Sect. 2.2, we will see that Eq. (1) can be actually realized at $\Lambda_{\rm MPP} = 10^{17}$ GeV.

One of the good features of this model is that electroweak symmetry breaking can be triggered by $U(1)_{B-L}$ symmetry breaking via the Coleman–Weinberg (CW) mechanism. In Ref. [26], it was argued that we can naturally obtain $v_h = \mathcal{O}(100)\,{\rm GeV}$ by imposing $\lambda(M_{\rm pl}) = 0$ and $\kappa(M_{\rm pl}) = 0$. Here, the important point is that $\lambda_\Psi(\Lambda_{\rm MPP}) \neq 0$ is needed to realize such $B-L$ breaking.[1] Therefore, if we try to combine this fact and the MPP, a natural question arises:

- *Is* $\mathcal{O}(100)$ *GeV electroweak symmetry breaking possible even if* $\lambda_\Psi(\Lambda_{\rm MPP})$ *is small?*

In Sect. 2.3, we will see that this is actually possible even if $\lambda_\Psi(\Lambda_{\rm MPP}) \leq 10^{-10}$. The reason for this is very simple: By tuning the parameters of the model, we can obtain the favorable scale at which $U(1)_{B-L}$ breaks so that v_h becomes $\mathcal{O}(100)\,{\rm GeV}$. Therefore, the $B-L$ model is a phenomenologically very interesting model in that it can explain the natural-scale electroweak symmetry breaking while satisfying the (slightly broken) MPP. Furthermore, within this situation, we find that the mass of the $B-L$ gauge boson is predicted to be

$$M_{B-L} = 2g_{B-L}(v_{B-L})v_{B-L} = 2\sqrt{2} \times \sqrt{\frac{\lambda(v_h)}{0.10}} \times v_h \simeq 696\,{\rm GeV}, \tag{3}$$

where v_{B-L} is the expectation value of Ψ and we have used the typical value $\lambda(v_h) \simeq 0.1$. This is a remarkable prediction of the (slightly broken) MPP, and it is surprising that the predicted value of M_{B-L} depends only on the SM parameters.[2]

On the other hand, there are many observational results from the cosmological side. One of the reliable possibilities to explain them is cosmic inflation. As is well known, Higgs inflation is possible in the SM where the criticality of the Higgs potential plays an important role in realizing the inflation naturally [17]. Of course, such a Higgs inflation is possible in the $B-L$ model, but we can also consider the inflation scenario where Ψ plays the role of the inflaton [28]. In this paper, we

[1] Realizing $B-L$ symmetry breaking when $\lambda_\Psi(\Lambda_{\rm MPP}) = 0$ is difficult; see Sect. 2.

[2] Unfortunately, this value of M_{B-L} is already excluded by the ATLAS experiment [29]; see Sect. 2.3.

study $\lambda_\Psi \Psi^4$ inflation with non-minimal gravitational coupling $\xi \Psi^2 \mathcal{R}$. Our analysis is based on the following condition:

- *We consider inflation in the situation where the minimum of the Higgs potential vanishes at* $\Lambda_{\rm MPP} = 10^{17}$ GeV *and electroweak symmetry breaking occurs at* $\mathcal{O}(100)$ GeV.

In the following discussion, we will see that this condition strongly constrains the parameters, and, as a result, we can obtain unique cosmological predictions[3] that are consistent with the recent values observed by Planck [32] and BICEP2 [33].

This paper is organized as follows. In Sect. 2, we study the MPP and the $B - L$ symmetry breaking from the point of view of the slightly broken MPP. In Sect. 3, we investigate the inflation scenario where the SM singlet complex scalar Ψ plays the role of the inflaton. In Sect. 4, we give a summary.

2. MPP of the $B - L$ model and symmetry breaking

The flow of this section is as follows. In Sect. 2.1, we briefly review the gauged $B - L$ model. In Sect. 2.2, we consider the MPP of this model. In Sect. 2.3, we study whether $\mathcal{O}(100)$ GeV electroweak symmetry breaking can be realized even if λ_Ψ ($\Lambda_{\rm MPP}$) is very small.

2.1. *Short review of the $B - L$ model*

In this subsection, we briefly review the $B - L$ extension of the SM. Here, our discussion is mainly based on Ref. [30]. As mentioned in the introduction, this model can be obtained by gauging the global $\mathrm{U}(1)_{B-L}$ symmetry. The kinetic terms of the two U(1) gauge fields are given as follows:

$$\mathcal{L}_{\rm kin} = -\frac{1}{4} F^{\mu\nu} F_{\mu\nu} - \frac{1}{4} F^{\mu\nu}_{B-L} F_{B-L\mu\nu} - \frac{\omega}{4} F^{\mu\nu}_{B-L} F_{\mu\nu}, \tag{4}$$

where $\omega (\in \mathbb{R})$ represents the kinetic mixing. The U(1) part of the covariant derivative of a matter field ϕ_k is given by

$$\mathcal{D}_\mu = \partial_\mu + i \sum_{i=1}^{2} \sum_{j=1}^{2} Y^i_k g_{ij} A^j_\mu, \tag{5}$$

where A^1_μ and A^2_μ are the gauge fields of $\mathrm{U}(1)_Y$ and $\mathrm{U}(1)_{B-L}$, respectively, Y^i_k are the U(1) charges, and g_{ij} represent the U(1) gauge couplings. We can remove the mixing term by changing A^1_μ and A^2_μ to the new fields A^Y_μ and A^{B-L}_μ:

$$A^1_\mu = \frac{1}{\sqrt{2(1+\omega)}} A^Y_\mu + \frac{1}{\sqrt{2(1-2\omega)}} A^{B-L}_\mu, \quad A^2_\mu = \frac{1}{\sqrt{2(1+\omega)}} A^Y_\mu - \frac{1}{\sqrt{2(1-2\omega)}} A^{B-L}_\mu. \tag{6}$$

We simply express Eq. (6) as $A^i_\mu = \sum_\alpha R^i_\alpha A^\alpha_\mu$. By this transformation, the new gauge couplings are

$$g'_{i\alpha} := \sum_j g_{ij} R^j_\alpha. \tag{7}$$

We denote $g'_{i\alpha}$ as g_{YY}, g_{YE}, g_{EY}, and g_{EE} without a prime in the following discussion. Only three of them are meaningful because we can further rotate the gauge fields without producing

[3] Here, we use "unique" in the sense that our predictions do not strongly depend on the parameters of the model, except for λ_Ψ, ξ, and the initial value of Ψ.

the mixing term:

$$\begin{pmatrix} A^Y \\ A^{B-L} \end{pmatrix} = \begin{pmatrix} \cos\theta & -\sin\theta \\ \sin\theta & \cos\theta \end{pmatrix} \begin{pmatrix} \tilde{A}^Y \\ \tilde{A}^{B-L} \end{pmatrix}.$$

Thus, we can choose the angle θ so that one of $g_{\alpha\beta}$ vanishes. For convenience, we take the following bases:

$$B_\mu := \frac{g_{EE}A_\mu^{B-L} + g_{EY}A_\mu^Y}{\sqrt{g_{EE}^2 + g_{EY}^2}}, \quad E_\mu := \frac{-g_{EY}A_\mu^{B-L} + g_{EE}A_\mu^Y}{\sqrt{g_{EE}^2 + g_{EY}^2}}. \tag{8}$$

In these bases, the second term of Eq. (5) becomes

$$g_Y Y_k^Y B_\mu + \left(g_{B-L}Y_k^{B-L} + g_{\rm mix}Y_k^Y\right)E_\mu, \tag{9}$$

where

$$g_Y := \frac{g_{EE}g_{YY} - g_{EY}g_{YE}}{\sqrt{g_{EE}^2 + g_{EY}^2}}, \quad g_{B-L} := \sqrt{g_{EE}^2 + g_{EY}^2}, \quad g_{\rm mix} := \frac{g_{YE}g_{EE} + g_{EY}g_{YY}}{\sqrt{g_{EE}^2 + g_{EY}^2}}. \tag{10}$$

As a result, B_μ plays the role of the ordinary $\mathrm{U}(1)_Y$ gauge field, and E_μ is a new gauge field that can have a mass if the $B-L$ symmetry is broken. We use Eq. (9) for the calculations of the RGEs in Appendix A.

The particle contents (except for the gauge bosons) and their charges are presented in Table 1. In addition to the SM particles, there are three right-handed neutrinos and a SM singlet complex scalar whose $\mathrm{U}(1)_{B-L}$ charge is $+2$. The relevant terms of the renormalizable Lagrangian are

$$\begin{aligned} \mathcal{L} \supset & -\lambda\left(H^\dagger H\right)^2 - \lambda_\Psi\left(\Psi^\dagger\Psi\right)^2 - \kappa\left(H^\dagger H\right)\left(\Psi^\dagger\Psi\right) \\ & - \sum_{ij} y_\nu^{ij}\bar{\nu}_R^i H^\dagger \ell_L^j - \frac{1}{2}\sum_{ij} Y_R^{ij}\bar{\nu^c}_R^i \nu_R^j \Psi + \text{h.c.} \end{aligned} \tag{11}$$

In the following discussion, we use the bases such that y_ν^{ij} and Y_R^{ij} are real and diagonalized, and assume that they are equal, respectively, for the three generations. As a result, by including the top mass M_t, there are seven unknown parameters in this model:

$$M_t, \quad g_{B-L}, \quad g_{\rm mix}, \quad \lambda_\Psi, \quad \kappa, \quad y_\nu, \quad Y_R. \tag{12}$$

If we assume that small neutrino masses ($\lesssim$1 eV) are generated by the ordinary seesaw mechanism triggered by $\mathrm{U}(1)_{B-L}$ symmetry breaking at a low-energy scale $\left(\ll 10^{13}\,\text{GeV}\right)$, y_ν should be very small, and its effects on the RGEs are negligible. In this paper, we assume such a situation.

2.2. *Multiple point principle*

To understand how these couplings behave at a high-energy scale, we need to know the RGEs. The two-loop RGEs of this model are presented in Appendix A. Furthermore, the one-loop effective

Table 1. The particle contents of the $B-L$ model and their charges except for the gauge bosons. Here, i represents the generation.

	$SU(3)_c$	$SU(2)_L$	$U(1)_Y$	$U(1)_{B-L}$
Q_L^i	**3**	**2**	$+1/6$	$+1/3$
u_R^i	**3**	**1**	$+2/3$	$+1/3$
d_R^i	**3**	**1**	$-1/3$	$+1/3$
ℓ_L^i	**1**	**2**	$-1/2$	-1
ν_R^i	**1**	**1**	0	-1
e_R^i	**1**	**1**	-1	-1
H	**1**	**2**	$-1/2$	0
Ψ	**1**	**1**	0	$+2$

potentials in the Landau gauge are as follows:[4]

$$V_{\rm eff}^H(\mu,\phi)=\frac{\lambda(\mu)}{4}\phi^4+V_{1-\rm loop}^H(\mu,\phi),\ V_{\rm eff}^\Psi(\mu,\Psi)=\frac{\lambda_\Psi(\mu)}{4}\Psi^4+V_{1-\rm loop}^\Psi(\mu,\Psi), \tag{13}$$

$$\begin{aligned}V_{1-\rm loop}^H(\mu,\phi):=e^{4\Gamma(\mu)}\Bigg\{&-12\cdot\frac{M_t(\phi)^4}{64\pi^2}\left[\log\left(\frac{M_t(\phi)^2}{\mu^2}\right)-\frac{3}{2}+2\Gamma(\mu)\right]\\&+6\cdot\frac{M_W(\phi)^4}{64\pi^2}\left[\log\left(\frac{M_W(\phi)^2}{\mu^2}\right)-\frac{5}{6}+2\Gamma(\mu)\right]\\&+3\cdot\frac{M_Z(\phi)^4}{64\pi^2}\left[\log\left(\frac{M_Z(\phi)^2}{\mu^2}\right)-\frac{5}{6}+2\Gamma(\mu)\right]\Bigg\},\\V_{1-\rm loop}^\Psi(\mu,\Psi):=e^{4\Gamma_\Psi(\mu)}\Bigg\{&-6\cdot\frac{M_R(\Psi)^4}{64\pi^2}\left[\log\left(\frac{M_R(\Psi)^2}{\mu^2}\right)-\frac{3}{2}+2\Gamma_\Psi(\mu)\right]\\&+3\cdot\frac{M_{B-L}(\Psi)^4}{64\pi^2}\left[\log\left(\frac{M_{B-L}(\Psi)^2}{\mu^2}\right)-\frac{5}{6}+2\Gamma_\Psi(\mu)\right]\Bigg\},\end{aligned} \tag{14}$$

where

$$\begin{aligned}&M_t(\phi)=\frac{y_t(\mu)}{\sqrt{2}}\phi,\quad M_W(\phi)=\frac{g_2(\mu)}{2}\phi,\quad M_Z(\phi)=\frac{\sqrt{g_2^2(\mu)+g_{\rm Y}^2(\mu)}}{2}\phi,\\&M_R(\Psi)=\frac{Y_R(\mu)}{\sqrt{2}}\Psi,\quad M_{B-L}(\Psi)^2=2^2g_{B-L}(\mu)^2\Psi^2.\end{aligned} \tag{15}$$

Here, μ is the renormalization scale and Γ, Γ_Ψ are the wave function renormalizations. To minimize the one-loop contributions, we take $\mu=\phi\,(\Psi)$ in the following discussion.[5] From these results, we

[4] Here, we neglect the one-loop contributions that include λ, λ_Ψ, and κ because their effects are very small when we consider the MPP.

[5] Precisely speaking, μ should be determined as a function of ϕ and Ψ by minimizing the one-loop effective potential. However, in this paper, we simply choose $\mu=\phi\,(\Psi)$ when we focus on $\lambda^{\rm eff}$ ($\lambda_\Psi^{\rm eff}$). It is known that this choice is a good approximation [17].

can define the effective self-couplings and their effective beta functions as follows:

$$\lambda^{\rm eff}(\phi) := \frac{4V^H_{\rm eff}(\phi)}{\phi^4}, \quad \beta^{\rm eff}_\lambda := \frac{d\lambda^{\rm eff}(\phi)}{d\ln\phi}, \tag{16}$$

$$\lambda^{\rm eff}_\Psi(\Psi) := \frac{4V^\Psi_{\rm eff}(\Psi)}{\Psi^4}, \quad \beta^{\rm eff}_{\lambda_\Psi} := \frac{d\lambda^{\rm eff}_\Psi(\Psi)}{d\ln\Psi}. \tag{17}$$

Figure 1 shows the typical behaviors of $\lambda^{\rm eff}(\phi)$ and its parameter dependences. Here, for later convenience, the initial values of λ_Ψ, κ, g_{B-L}, $g_{\rm mix}$, and Y_R are given at $\Lambda_{\rm MPP} = 10^{17}$ GeV, and their typical values are chosen to be 0.1, respectively. One can see that $\lambda^{\rm eff}(\phi)$ depends weakly on g_{B-L} and Y_R because they appear in β_λ at the two-loop level.

Now, let us consider the MPP. By including the top mass M_t and neglecting y_ν, there are six parameters in this model:

$$M_t, \quad g_{B-L}, \quad g_{\rm mix}, \quad \lambda_\Psi, \quad \kappa, \quad Y_R. \tag{18}$$

Therefore, in principle, they are uniquely determined by the MPP conditions:

$$\lambda^{\rm eff}(\Lambda_{\rm MPP}) = \lambda^{\rm eff}_\Psi(\Lambda_{\rm MPP}) = \kappa(\Lambda_{\rm MPP}) = \beta^{\rm eff}_\lambda(\Lambda_{\rm MPP}) = \beta^{\rm eff}_{\lambda_\Psi}(\Lambda_{\rm MPP}) = \beta_\kappa(\Lambda_{\rm MPP}) = 0. \tag{19}$$

Among these, $\lambda^{\rm eff}_\Psi(\Lambda_{\rm MPP}) = \kappa(\Lambda_{\rm MPP}) = 0$ are just the initial conditions of λ_Ψ and κ, and other conditions give us constraints between the remaining parameters. We can understand such constraints qualitatively from the one-loop RGEs:

- $\beta^{\rm eff}_\lambda(\Lambda_{\rm MPP}) = 0$ mainly relates M_t and $g_{\rm mix}$ because they appear in β_λ at the one-loop level (see Eq. (A12) in Appendix A). As a result, we can fix M_t and $g_{\rm mix}$ by $\lambda^{\rm eff}(\Lambda_{\rm MPP}) = \beta^{\rm eff}_\lambda(\Lambda_{\rm MPP}) = 0$. They are

$$171.74\,{\rm GeV} \le M_t \le 171.82\,{\rm GeV}, \quad 0.21 \le g_{\rm mix}(\Lambda_{\rm MPP}) \le 0.27, \tag{20}$$

  according to $0 \le g_{B-L}(\Lambda_{\rm MPP}) \le 0.4$.[6]
- We can obtain a relation between $g_{B-L}(\Lambda_{\rm MPP})$ and $Y_R(\Lambda_{\rm MPP})$ by $\beta_{\lambda_\Psi}(\Lambda_{\rm MPP}) = 0$ because the one-loop part of β_{λ_Ψ} at $\Lambda_{\rm MPP}$ is

$$\beta_{\lambda_\Psi}|_{1-{\rm loop}}(\Lambda_{\rm MPP}) = \frac{1}{16\pi^2}\left(96g^4_{B-L} - 3Y^4_R\right). \tag{21}$$

- Finally, $g_{B-L}(\Lambda_{\rm MPP})$ (or $Y_R(\Lambda_{\rm MPP})$) can be fixed at 0 by $\beta_\kappa(\Lambda_{\rm MPP}) = 0$ because the one-loop part of β_κ at $\Lambda_{\rm MPP}$ is

$$\beta_\kappa|_{1-{\rm loop}}(\Lambda_{\rm MPP}) = \frac{1}{16\pi^2}\left(12g^2_{B-L}g^2_{\rm mix} - 12Y^2_R y^2_\nu\right) \simeq \frac{12g^2_{B-L}g^2_{\rm mix}}{16\pi^2}. \tag{22}$$

In Fig. 2, we show the effective potentials (upper) and the runnings (lower) of $\lambda^{\rm eff}_\Psi$ and κ that satisfy the above MPP conditions. Here, in the lower panels, we leave $g_{B-L}(\Lambda_{\rm MPP})$ as a free parameter. One can see that the flat potentials can be actually realized at $\Lambda_{\rm MPP}$.

Summary: From the MPP at $\Lambda_{\rm MPP} = 10^{17}$ GeV, the parameters of the gauged $B-L$ extension of the SM are fixed at

$$\begin{aligned} &M_t \simeq 171.8\,{\rm GeV}, \quad g_{B-L}(\Lambda_{\rm MPP}) \simeq 0, \quad g_{\rm mix}(\Lambda_{\rm MPP}) \simeq 0.2, \\ &\lambda_\Psi(\Lambda_{\rm MPP}) \simeq 0, \quad \kappa(\Lambda_{\rm MPP}) \simeq 0, \quad Y_R(\Lambda_{\rm MPP}) \simeq 0. \end{aligned} \tag{23}$$

[6] $Y_R(\Lambda_{\rm MPP})$ dependence is negligible.

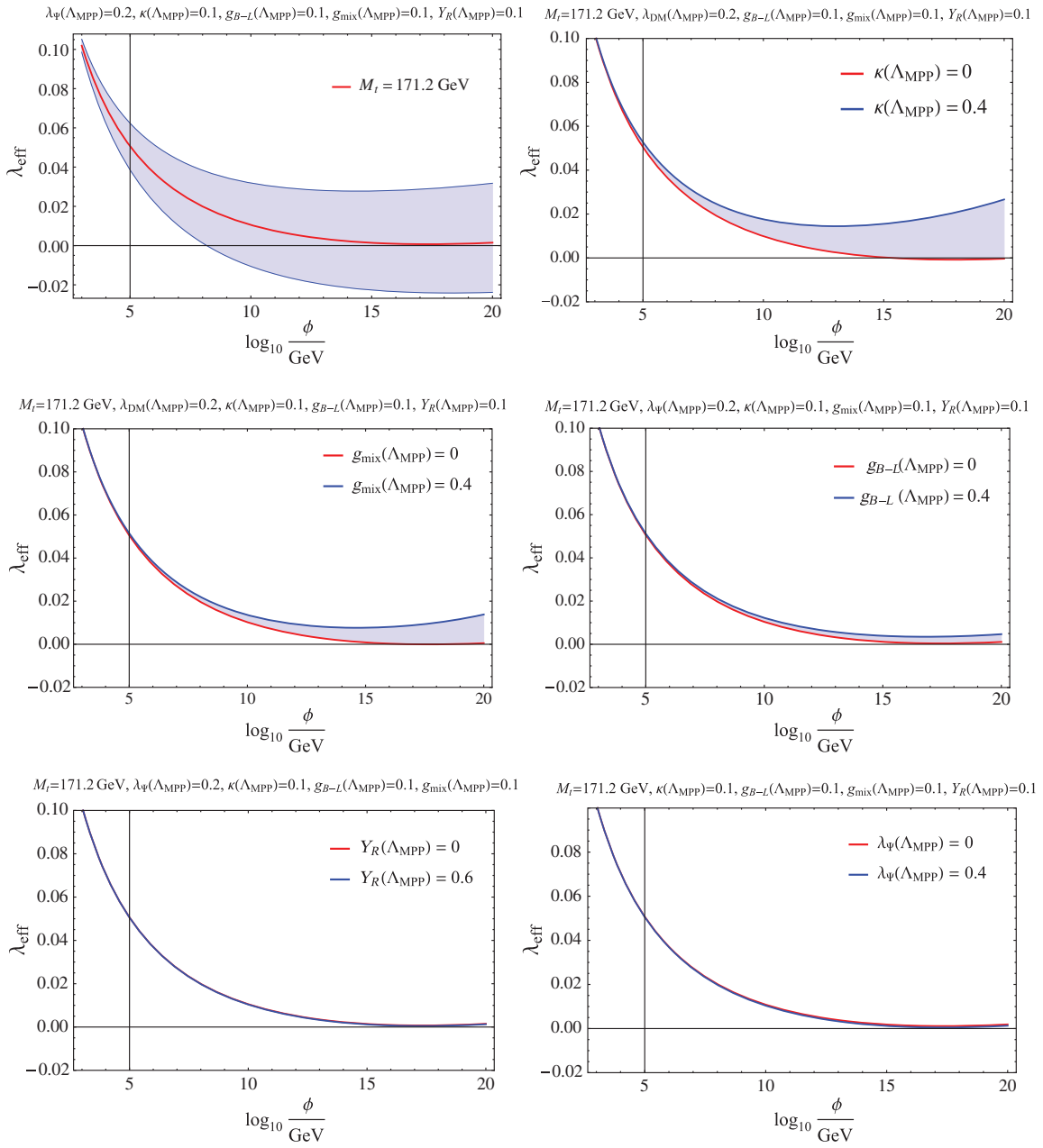

Fig. 1. The runnings of the Higgs effective self-coupling $\lambda_{\rm eff}$ as a function of ϕ. The upper-left (-right) panel shows the M_t $\left(\kappa\left(\Lambda_{\rm MPP}\right)\right)$ dependence. In the case of M_t, the blue band corresponds to 95% CL deviation from 171.2 GeV. The middle-left (-right) panel shows the $g_{\rm mix}\left(\Lambda_{\rm MPP}\right)$ $\left(g_{B-L}\left(\Lambda_{\rm MPP}\right)\right)$ dependence. The lower-left (-right) panel shows the $Y_R\left(\Lambda_{\rm MPP}\right)$ $\left(\lambda_\Psi\left(\Lambda_{\rm MPP}\right)\right)$ dependence.

2.3. *Electroweak symmetry breaking by breaking the MPP*

We first explain how electroweak symmetry breaking is triggered by $B-L$ symmetry breaking. If Ψ has an expectation value $\langle\Psi\rangle := v_{B-L}/\sqrt{2}$, the interaction term $-\kappa\left(H^\dagger H\right)\left(\Psi^\dagger\Psi\right)$ produces the mass term of H:

$$\mathcal{L} \ni -\frac{\kappa}{2}v_{B-L}^2 H^\dagger H. \tag{24}$$

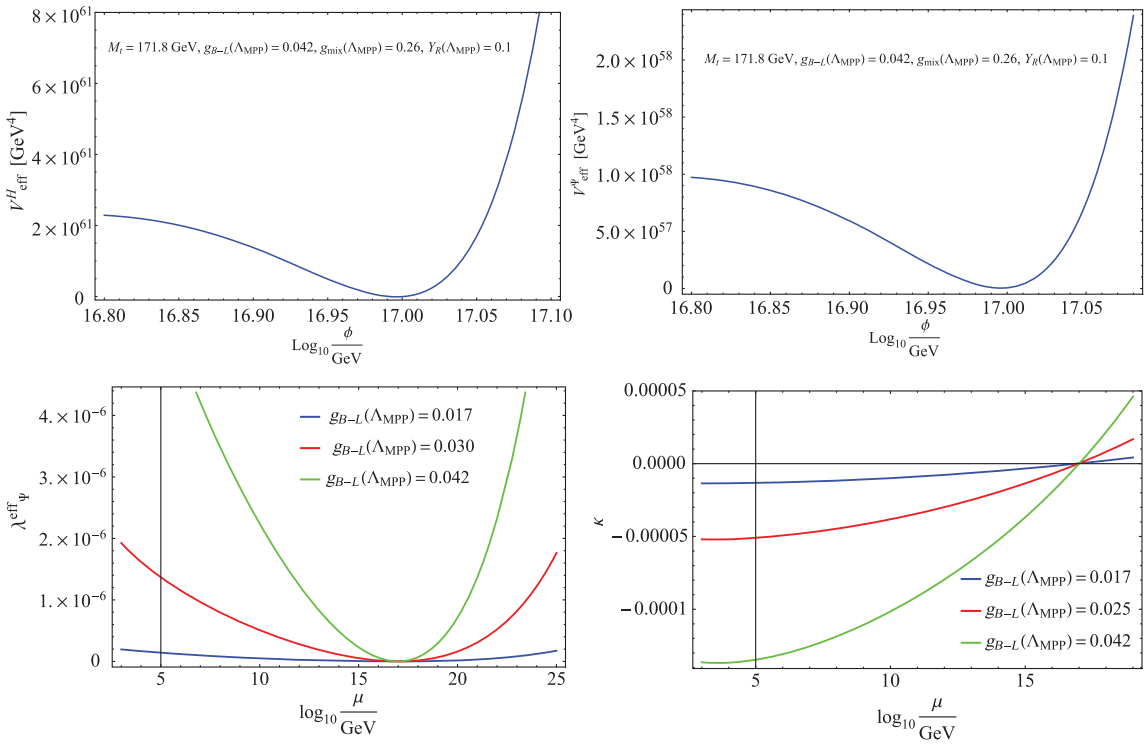

Fig. 2. The effective potentials (upper) and the runnings of $\lambda^{\rm eff}_\Psi$ and κ that satisfy the MPP conditions (lower). The upper-left (-right) panel shows $V^H_{\rm eff}\left(V^\Psi_{\rm eff}\right)$. They are exactly flat at $\Lambda_{\rm MPP} = 10^{17}$ GeV. In the lower panels, we leave $g_{B-L}\left(\Lambda_{\rm MPP}\right)$ as a free parameter. The different colors correspond to the different values of $g_{B-L}\left(\Lambda_{\rm MPP}\right)$.

Thus, if κ is negative at the $B-L$ breaking scale, electroweak symmetry breaking occurs, and the corresponding Higgs expectation value v_h is given by

$$v_h = \sqrt{-\frac{\kappa}{2\lambda}} \times v_{B-L}\Big|_{\mu=v_h}. \tag{25}$$

This is a relation between v_h and v_{B-L}. We must consider a few questions to realize electroweak symmetry breaking at $\mathcal{O}(100)$ GeV:

Question 1: Does $B-L$ symmetry breaking actually occur? In particular, is it possible to realize it in the situation where the MPP is exactly satisfied?

See the lower-left panel of Fig. 2 once again. This shows the running of $\lambda^{\rm eff}_\Psi$ when the MPP conditions are satisfied. One can see that $\lambda^{\rm eff}_\Psi$ is a monotonically decreasing function in the $\mu \leq \Lambda_{\rm MPP}$ region. Thus, we cannot obtain $B-L$ symmetry breaking if the MPP is realized exactly. However, as discussed in Ref. [26], the situation changes when $\lambda^{\rm eff}_\Psi\left(\Lambda_{\rm MPP}\right) > 0$ and $\beta^{\rm eff}_{\lambda_\Psi}\left(\Lambda_{\rm MPP}\right) > 0$, which mean the breaking of the MPP. See the upper- and middle-left panels of Fig. 3. They show the runnings of $\lambda^{\rm eff}_\Psi$ when $\lambda^{\rm eff}_\Psi\left(\Lambda_{\rm MPP}\right) = 10^{-10}$ and 10^{-12}, respectively.[7] One can see that $\lambda^{\rm eff}_\Psi$ can cross zero, and its scale strongly depends on $g_{B-L}\left(\Lambda_{\rm MPP}\right)$. For convenience, we also show the corresponding effective potentials of Ψ in the upper- and middle-right panels. Here, we have normalized the vertical axes so that the minimums of the potentials can be easily understood. In the following discussion,

[7] In Sect. 3, we will see that $\lambda^{\rm eff}_\Psi$ is required to be small to explain the cosmological observations. This is why we have chosen $\lambda^{\rm eff}_\Psi$ to be so small here.

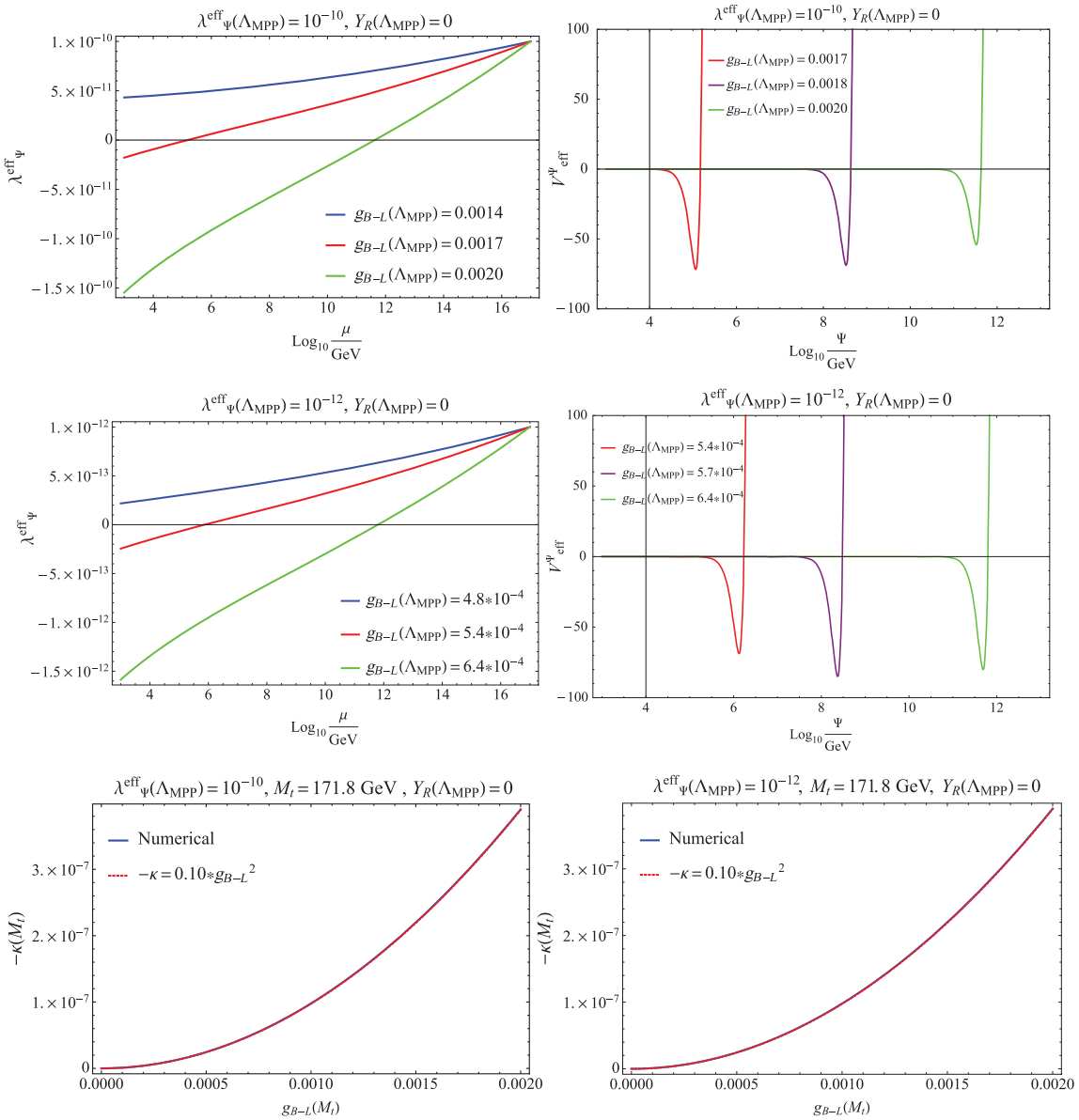

Fig. 3. Upper (middle): the runnings of $\lambda^{\rm eff}_\Psi$ (left) and the corresponding effective potentials (right) in the case of $\lambda^{\rm eff}_\Psi(\Lambda_{\rm MPP}) = 10^{-10}$ (10^{-12}). Here, the vertical axes of the right panels are properly normalized. The different colors correspond to the different values of $g_{B-L}(\Lambda_{\rm MPP})$. Lower-left (-right): κ vs g_{B-L} at $M_t = 171.8$ GeV for $\lambda^{\rm eff}_\Psi(\Lambda_{\rm MPP}) = 10^{-10}$ (10^{-12}). Here, the solid blue lines are the numerical results of the RGEs, and the dashed red contours represent $-\kappa = 0.10 \times g^2_{B-L}$.

besides $\lambda^{\rm eff}_\Psi(\Lambda_{\rm MPP}) > 0$ and $\beta_{\lambda^{\rm eff}_\Psi}(\Lambda_{\rm MPP}) > 0$, we consider the situation such that only $\lambda^{\rm eff}$, $\beta^{\rm eff}_\lambda$, and κ satisfy the MPP conditions:

$$\lambda^{\rm eff}(\Lambda_{\rm MPP}) = \beta^{\rm eff}_\lambda(\Lambda_{\rm MPP}) = \kappa(\Lambda_{\rm MPP}) = 0$$
$$\lambda^{\rm eff}_\Psi(\Lambda_{\rm MPP}) > 0, \quad \beta^{\rm eff}_{\lambda_\Psi}(\Lambda_{\rm MPP}) > 0, \quad \beta_\kappa(\Lambda_{\rm MPP}) > 0. \tag{26}$$

Question 2: Although we have seen that $B - L$ symmetry breaking is possible if we break the MPP, is it possible to realize $v_h = \mathcal{O}(100)$ GeV?

To answer this question, we should know the typical values of κ at a low-energy scale (see Eq. (25)). Before seeing the numerical results, let us understand them qualitatively. Because we now consider

the MPP, the one-loop part of β_κ approximately becomes (see Eq. (A13) in Appendix A)

$$\beta_\kappa|_{1-\text{loop}} \simeq \frac{12 g_{B-L}^2 g_{\text{mix}}^2}{16\pi^2} \simeq \frac{g_{B-L}^2}{\pi} \times 10^{-2}, \tag{27}$$

where we have used $g_{\text{mix}} \simeq 0.2$, which was obtained from $\lambda^{\text{eff}}(\Lambda_{\text{MPP}}) = \beta_\lambda^{\text{eff}}(\Lambda_{\text{MPP}}) = 0$. Thus, κ at a low-energy scale μ is approximately given by

$$-\kappa(\mu) = c \times 0.1 \times g_{B-L}^2(\mu), \tag{28}$$

where c is a constant and we have used the fact that g_{B-L} does not change significantly.
This is the qualitative expression of $\kappa(\mu)$. In the lower-left (-right) panel of Fig. 3, we show κ vs g_{B-L} at $\mu = M_t = 171.8$ GeV in the case of $\lambda_\Psi^{\text{eff}}(\Lambda_{\text{MPP}}) = 10^{-10}$ (10^{-12}). One can see that Eq. (28) nicely explains the numerical results when c is 1.0. As a result, v_h is given by

$$v_h = \sqrt{\frac{0.1 \times c \times g_{B-L}(v_h)^2}{2\lambda(v_h)}} \times v_{B-L} \simeq g_{B-L}(v_h) v_{B-L}, \tag{29}$$

where we have used the typical value $\lambda(v_h) \simeq 0.1$. Therefore, we can obtain $v_h = \mathcal{O}(100)$ GeV by tuning $g_{B-L}(\Lambda_{\text{MPP}})$ and $Y_R(\Lambda_{\text{MPP}})$ so that the right-hand side of Eq. (29) becomes $\mathcal{O}(100)$ GeV. The red lines of the upper- and middle-left panels of Fig. 3 show such examples. In the upper (lower) case, g_{B-L} is $\mathcal{O}(10^{-3}(10^{-4}))$ and v_{B-L} is $\mathcal{O}(10^2(10^3))$ TeV.

A few comments are needed. First, because we no longer impose the flatness of V_{eff}^Ψ, the two parameters $g_{B-L}(\Lambda_{\text{MPP}})$ and $Y_R(\Lambda_{\text{MPP}})$ remain as free parameters. However, the parameter region that can produce $v_h = \mathcal{O}(100)$ GeV is quite limited. For example, in the $\lambda_\Psi^{\text{eff}}(\Lambda_{\text{MPP}}) = 10^{-10}$ case, it is

$$1.6 \times 10^{-3} \lesssim g_{B-L}(\Lambda_{\text{MPP}}) \lesssim 3.2 \times 10^{-3}, \tag{30}$$

and $Y_R(\Lambda_{\text{MPP}})$ is correspondingly fixed so that $\lambda_\Psi^{\text{eff}}$ crosses zero around $\mathcal{O}(100)$ TeV. The reason for this is as follows. When $g_{B-L}(\Lambda_{\text{MPP}})$ is small, β_{λ_Ψ} is too small to make $\lambda_\Psi^{\text{eff}}$ negative at a low-energy scale. As a result, $B-L$ symmetry breaking does not occur. On the other hand, when $g_{B-L}(\Lambda_{\text{MPP}})$ is too large, $B-L$ symmetry breaking occurs at a very high-energy scale. We can actually see these behaviors from Fig. 4. Note that the allowed values of $g_{B-L}(\Lambda_{\text{MPP}})$ become small when we decrease $\lambda_\Psi^{\text{eff}}(\Lambda_{\text{MPP}})$.

Second, g_{B-L} at a low-energy scale does not change very much from the value at Λ_{MPP}. See Fig. 5. This shows the typical runnings of g_{B-L} when $\lambda_\Psi^{\text{eff}}(\Lambda_{\text{MPP}}) = 10^{-10}$.

Finally, when Eq. (26) is satisfied, the mass of the $B-L$ gauge boson is uniquely predicted to be

$$M_{B-L} = 2 g_{B-L}(v_{B-L}) v_{B-L} = 2\sqrt{2} \times \sqrt{\frac{\lambda(v_h)}{0.10}} \times v_h, \tag{31}$$

where we have used Eq. (29) and $c = 1.0$. By using the experimental value $v_h = 246$ GeV and the typical value $\lambda(v_h) \simeq 0.1$, this leads to

$$M_{B-L} \simeq 696\,\text{GeV}. \tag{32}$$

Although this is a remarkable prediction of the MPP, this value is already excluded by the ATLAS experiment [29] because g_{mix} is too large.[8]

[8] In Ref. [29], g_{mix} is represented by $\tilde{g}_Y$. Therefore, $g_{\text{mix}} \simeq 0.24$ corresponds to the contour $\gamma' \simeq 0.32/\sin\theta$ in Fig. 7 of Ref. [29].

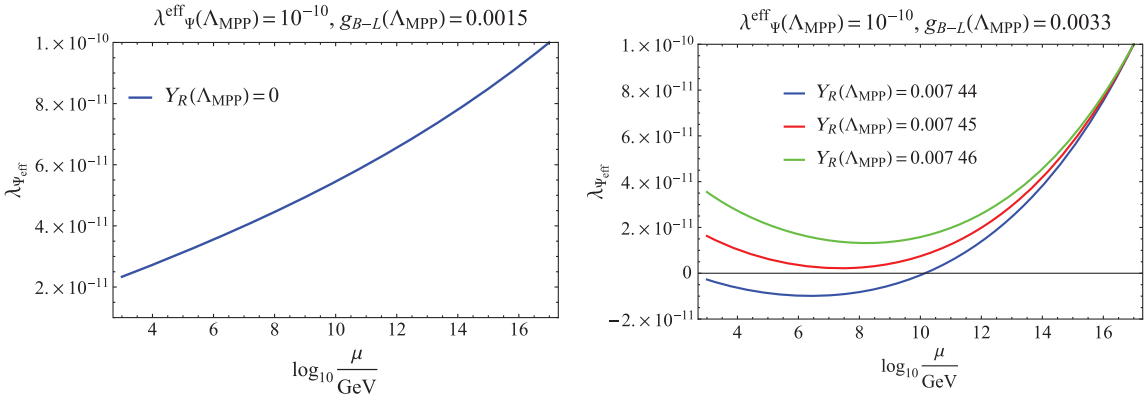

Fig. 4. The impossibility of realizing $v_h = \mathcal{O}(100)$ GeV when $g_{B-L}(\Lambda_{\rm MPP})$ is outside the region given by Eq. (30). The left (right) panel shows the running of $\lambda_\Psi^{\rm eff}$ when $g_{B-L}(\Lambda_{\rm MPP}) = 0.0015\,(0.0033)$. In the left panel, one can see that $\lambda_\Psi^{\rm eff}$ is always positive even if $Y_R(\Lambda_{\rm MPP}) = 0$. In the right panel, one can see that $B-L$ symmetry breaking occurs at a very high-energy scale ($\gg 10^2$ TeV).

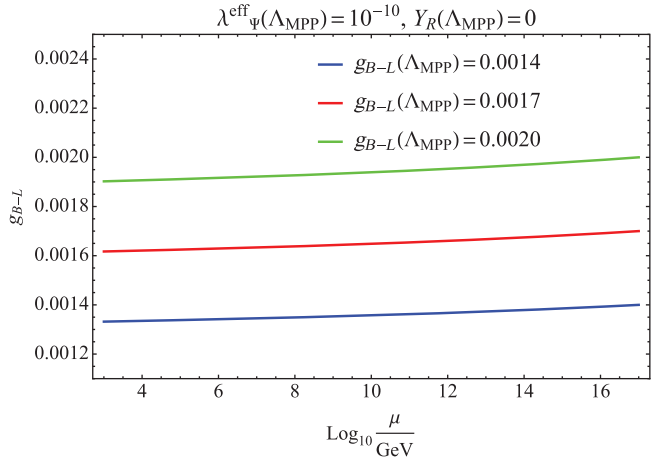

Fig. 5. The typical runnings of g_{B-L} when $\lambda_\Psi^{\rm eff}(\Lambda_{\rm MPP}) = 10^{-10}$.

3. Non-minimal inflation: The SM singlet scalar as the inflaton

As is well known, Higgs inflation is possible in the SM [14–18]. There, the criticality of the Higgs potential plays a crucial role in realizing inflation naturally; we can obtain sufficient e-foldings and cosmic microwave background (CMB) fluctuations even if ξ is $\mathcal{O}(1)$ by making the running Higgs self-coupling arbitrarily small (see Ref. [17] for more details). In other words, the smallness of the self-coupling is needed to realize the inflation naturally. Such a Higgs inflation is, of course, possible in our $B-L$ model; however, the conclusion of the previous section indicates a new possibility: The newly introduced SM singlet complex scalar Ψ plays the role of the inflaton [28]. We study this scenario in this section.

The action with the non-minimal gravitational coupling $\xi\Psi^2\mathcal{R}$ in the Jordan frame is given by

$$S_J = \int d^4x\sqrt{-g}\left\{-\left(\frac{M_{\rm pl}^2 + \xi\Psi^2}{2}\right)\mathcal{R} + \frac{1}{2}g^{\mu\nu}\partial_\mu\Psi\partial_\nu\Psi - \frac{\lambda_\Psi^{\rm eff}(\Psi)}{4}\Psi^4 + \cdots\right\}, \qquad (33)$$

where Ψ is the physical (real) field, and we have written the relevant terms for later discussion. To study the inflation, it is convenient to move to the Einstein frame. Namely, by the conformal

transformation

$$g^{\rm E}_{\mu\nu} := \Omega^2 g_{\mu\nu}, \quad \Omega^2 := 1 + \frac{\xi\Psi^2}{M_{\rm pl}^2}, \tag{34}$$

and the field redefinition

$$\frac{d\chi}{d\Psi} = \sqrt{\frac{\Omega^2 + 6\xi^2\Psi^2/M_{\rm pl}^2}{\Omega^4}}, \tag{35}$$

the action becomes

$$S_E = \int d^4x\sqrt{-g_E}\left\{-\frac{M_{\rm pl}^2}{2}\mathcal{R}_E + \frac{1}{2}g_E^{\mu\nu}\partial_\mu\chi\partial_\nu\chi - \frac{\lambda_\Psi^{\rm eff}(\Psi)}{4\Omega^4}\Psi^4(\chi) + \cdots\right\}. \tag{36}$$

This is the canonically normalized form, and the potential in this frame is given by

$$U(\chi) := \frac{\lambda_\Psi^{\rm eff}(\Psi)}{4\Omega^4}\Psi^4(\chi). \tag{37}$$

For large values of $\Psi \gg M_{\rm pl}/\sqrt{\xi}$, Eq. (35) becomes

$$\frac{d\chi}{d\Psi} \simeq \frac{M_{\rm pl}}{\Psi}\sqrt{\frac{1+6\xi}{\xi}}, \tag{38}$$

so we have

$$\Psi \simeq M_{\rm pl}\exp\left(\frac{\chi}{M_{\rm pl}\sqrt{(1+6\xi)/\xi}}\right). \tag{39}$$

In this limit, the potential in the Einstein frame, Eq. (37), becomes

$$U(\chi) \simeq \frac{\lambda_\Psi^{\rm eff}(\Psi)M_{\rm pl}^4}{4\xi^2}\left(1+\exp\left(-\frac{2\chi}{M_{\rm pl}\sqrt{(1+6\xi)/\xi}}\right)\right)^{-2}. \tag{40}$$

This is an exponentially flat potential (see, e.g., Fig. 6), so we can use the slow-roll approximations. The slow-roll parameters are

$$\epsilon := \frac{M_{\rm pl}^2}{2}\left(\frac{1}{U}\frac{dU}{d\chi}\right)^2 = \frac{M_{\rm pl}^2}{2}\left(\frac{d\Psi}{d\chi}\frac{U'}{U}\right)^2, \tag{41}$$

$$\eta := M_{\rm pl}^2\left(\frac{1}{U}\frac{d^2U}{d\chi^2}\right) = \frac{M_{\rm pl}^2}{U}\frac{d\Psi}{d\chi}\frac{d}{d\Psi}\left(\frac{d\Psi}{d\chi}U'\right), \tag{42}$$

$$\zeta^2 := M_{\rm pl}^4\frac{1}{U^2}\frac{d^3U}{d\chi^3}\frac{dU}{d\chi}, \tag{43}$$

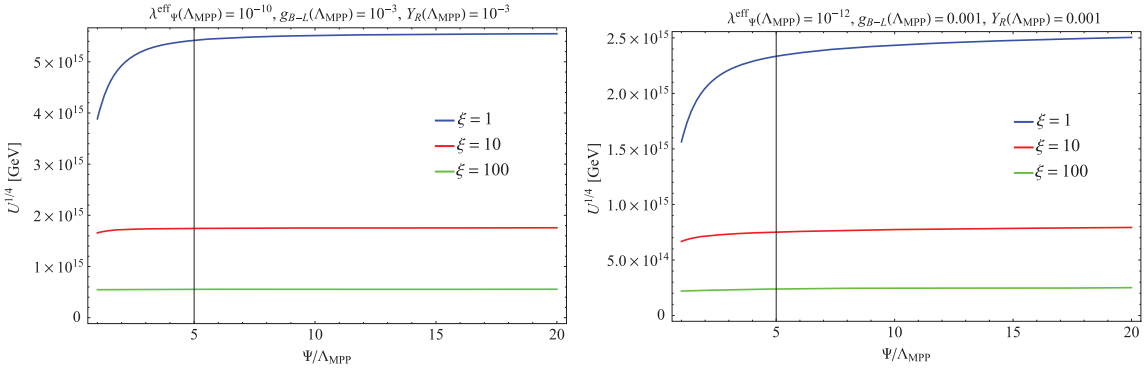

Fig. 6. The effective potentials in the Einstein frame. The left (right) panel shows the $\lambda_\Psi^{\rm eff}(\Lambda_{\rm MPP}) = 10^{-10}$ (10^{-12}) case. The different colors correspond to the different values of ξ.

where a prime represents a derivative with respect to Ψ. By using these quantities, the number of e-foldings N, the spectral index n_s, its running $dn_s/d\ln k$, and the tensor-to-scalar ratio r are given by

$$N = \int_{\chi_{\rm end}}^{\chi_{\rm ini}} d\chi \frac{1}{M_{\rm pl}^2}\frac{U}{dU/d\chi} = \int_{\Psi_{\rm end}}^{\Psi_{\rm ini}} d\Psi \frac{1}{M_{\rm pl}^2}\frac{U}{U'} \tag{44}$$

$$n_s = 1 - 6\epsilon + 2\eta, \tag{45}$$

$$\frac{dn_s}{d\ln k} = 16\epsilon\eta - 24\epsilon^2 - 2\zeta^2, \tag{46}$$

$$r = 16\epsilon, \tag{47}$$

where $\Psi_{\rm ini}$ ($\Psi_{\rm end}$) represents the initial (end) value of Ψ. In the following discussion, we denote $\Psi_{\rm ini}$ simply as Ψ.

Here, we give the current cosmological constraints by Planck TT + lowP [32]. The overall normalization of the CMB fluctuations at the scale $k_0 = 0.05\,{\rm Mpc}^{-1}$ is

$$A_s := \left.\frac{U}{24\pi^2\epsilon M_{\rm pl}^4}\right|_{k_0} = \left(2.198^{+0.076}_{-0.085}\right) \times 10^{-9}\ (68\%\ {\rm CL}), \tag{48}$$

and n_s, $dn_s/d\ln k$, and r are

$$n_s = 0.9655 \pm 0.0062\ (68\%\ {\rm CL}),\ \frac{dn_s}{d\ln k} = -0.0126^{+0.0098}_{-0.0087}\ (68\%\ {\rm CL}),\ r_{0.002} < 0.10\ (95\%\ {\rm CL}), \tag{49}$$

at the scale $k_0 = 0.05\,{\rm Mpc}^{-1}$ for n_s and $dn_s/d\ln k$, and $k_r = 0.002\,{\rm Mpc}^{-1}$ for $r_{0.002}$. On the other hand, the BICEP2 experiment has reported an observation of $r_{0.002}$ [33]:

$$r_{0.002} = 0.20^{+0.07}_{-0.05}\ (68\%\ {\rm CL}). \tag{50}$$

There has been discussion suggesting that this result may be consistent with $r = 0$ due to the foreground effect [34,35].

Our calculations are based on the following conditions:

(1) Although there are six parameters, we consider the situation where Eq. (26) is satisfied. Namely, M_t, $g_{\rm mix}(\Lambda_{\rm MPP})$, and $\kappa(\Lambda_{\rm MPP})$ are fixed, respectively, at 171.8 GeV, 0.2, and 0.

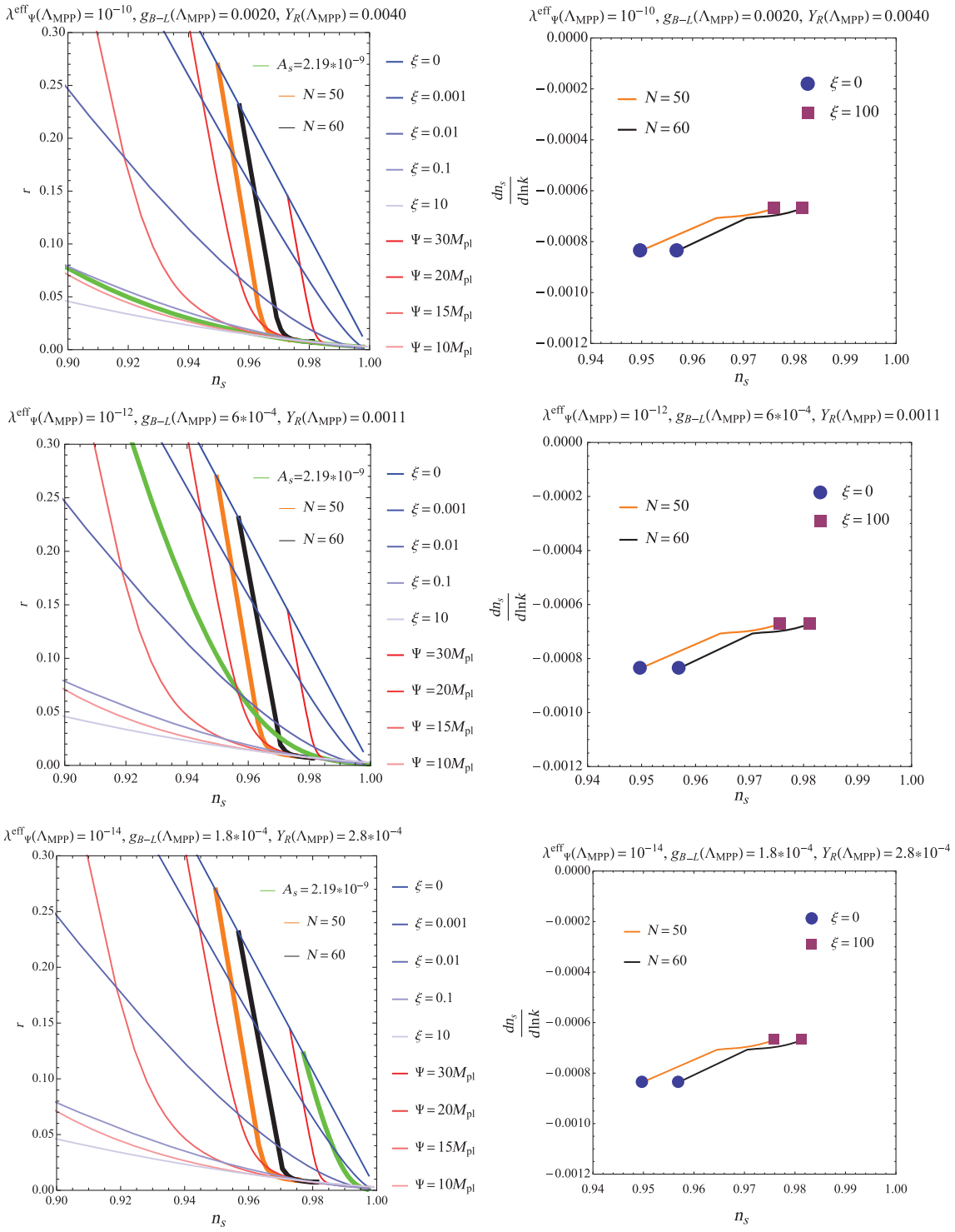

Fig. 7. The cosmological predictions of the gauged $B-L$ model. The upper, middle, and lower panels correspond to $\lambda^{\rm eff}_{\Psi}(\Lambda_{\rm MPP})=10^{-10}$, 10^{-12}, and 10^{-14}, respectively. The left (right) panels show n_s vs r ($dn_s/\ln k$). The blue (red) lines indicate that ξ (Ψ) = constant, and the contours that correspond to $N=50$ and 60 are represented by orange and black, respectively.

(2) As the typical values of $\lambda^{\rm eff}_{\Psi}(\Lambda_{\rm MPP})$, we choose

$$\lambda^{\rm eff}_{\Psi}(\Lambda_{\rm MPP})=10^{-10},\ 10^{-12},\ \text{and}\ 10^{-14}. \tag{51}$$

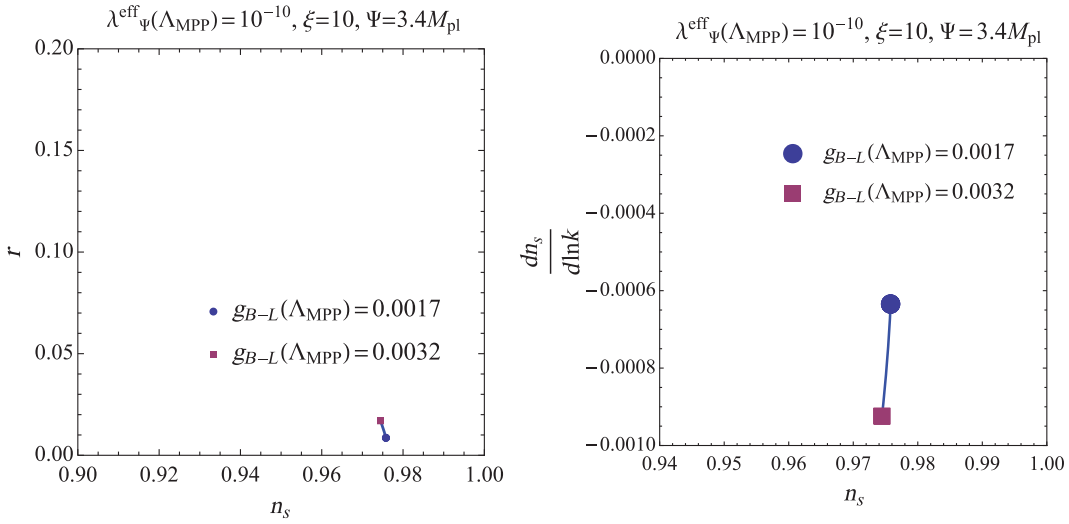

Fig. 8. The $g_{B-L}(\Lambda_{\rm MPP})$ dependences of n_s, r, and $dn_{s/\ln k}$. Here, we change $g_{B-L}(\Lambda_{\rm MPP})$ within the region such that electroweak symmetry breaking occurs at $\mathcal{O}(100)$ GeV, and ξ and Ψ are chosen so that both the observed value of A_s and $N = 50$ are satisfied when $g_{B-L}(\Lambda_{\rm MPP}) = 0.0020$. The left (right) panel shows r $(dn_s/\ln k)$ vs n_s.

(3) The remaining two parameters $g_{B-L}(\Lambda_{\rm MPP})$ and $Y_R(\Lambda_{\rm MPP})$ are chosen so that v_h becomes $\mathcal{O}(100)$ GeV. As discussed at the end of Sect. 2, the allowed region is quite limited in this case. We have checked that the cosmological predictions do not change very much even if we change these parameters within such a region (see Fig. 8).

Figure 7 shows our numerical results when we fix $g_{B-L}(\Lambda_{\rm MPP})$ and $Y_R(\Lambda_{\rm MPP})$. Our results are, of course, consistent with previous results such as Refs. [28,36]. The left (right) panels show r $(dn_s/\ln k)$ vs n_s. Here, the solid blue (red) lines represent ξ (Ψ) = constant, and the contours that correspond to $N = 50$ and 60 are represented by orange and black, respectively, from $\xi = 0$ to $\xi = 100$. In the left panels, we also show the contours of $A_s = 2.2 \times 10^{-9}$ in green. These results are consistent with the observed results (49) and (50) of Planck and BICEP2. In particular, as one can see from the behaviors of the green lines, the values of $\lambda_\Psi^{\rm eff}(\Lambda_{\rm MPP})$ that can simultaneously explain $A_s = 2.19 \times 10^{-9}$, sufficient e-foldings ($N \geq 50$), and the BICEP2 result $r = 0.2$ are quite limited:

$$10^{-14} < \lambda_\Psi^{\rm eff}(\Lambda_{\rm MPP}) < 10^{-12}. \tag{52}$$

Among the three quantities n_s, r, and $dn_s/\ln k$, one might think that the predicted values of $dn_s/\ln k$ are small compared with the observed values $\mathcal{O}(-0.01)$. It might be possible to improve this situation by including a higher-dimensional operator; see, e.g., Ref. [17].

In Fig. 8, we also show how n_s, r, and $dn_s/\ln k$ depend on $g_{B-L}(\Lambda_{\rm MPP})$ when $\lambda_\Psi^{\rm eff}(\Lambda_{\rm MPP}) = 10^{-10}$. Here, we change $g_{B-L}(\Lambda_{\rm MPP})$ within the region such that electroweak symmetry breaking occurs at $\mathcal{O}(100)$ GeV. Furthermore, Ψ and ξ are chosen so that they explain both the observed value of A_s and $N = 50$ when $g_{B-L}(\Lambda_{\rm MPP}) = 0.0020$. One can see that n_s and r hardly depend on $g_{B-L}(\Lambda_{\rm MPP})$ and that the change in $dn_s/\ln k$ is at most $\mathcal{O}(0.0001)$. As a result, in the situation where the minimum of the Higgs potential vanishes at $\Lambda_{\rm MPP}$ and electroweak symmetry breaking occurs at $\mathcal{O}(100)$ GeV, the gauged $B - L$ model uniquely predicts the cosmological observables. This is also one of the benefits of the (slightly broken) MPP.

4. Summary

In this paper, we have considered the MPP and the inflation of the gauged $B-L$ extension of the SM. We have found that the scalar couplings and their beta functions can simultaneously become zero at $\Lambda_{\rm MPP}=10^{17}$ GeV and that the parameters of the model can be uniquely fixed by these conditions. However, from the point of view that electroweak symmetry breaking should be realized by radiatively broken $B-L$ symmetry, it is necessary to break the MPP: we need $\lambda_\Psi^{\rm eff}(\Lambda_{\rm MPP})>0$ and $\beta_{\lambda_\Psi^{\rm eff}}(\Lambda_{\rm MPP})>0$. In Sect. 2.3, we found that small values of $\lambda_\Psi^{\rm eff}(\Lambda_{\rm MPP})$ are compatible with electroweak symmetry breaking at $\mathcal{O}(100)$ GeV. In particular, we have found that the mass of the $B-L$ gauge boson can be predicted to be

$$M_{B-L}=2\sqrt{2}\times\sqrt{\frac{\lambda(v_h)}{0.10}}\times v_h \tag{53}$$

from the MPP of the Higgs potential and κ. This is one of the remarkable predictions of the MPP. In Sect. 3, we have studied inflation, where the SM singlet scalar Ψ plays the role of the inflaton. We have calculated the cosmological observables based on the assumptions that the minimum of the Higgs potential vanishes at $\Lambda_{\rm MPP}=10^{17}$ GeV and electroweak symmetry breaking occurs at $\mathcal{O}(100)$ GeV. The results in this paper are consistent with the observations by Planck and BICEP2. Among these, the predicted values of the running of the spectral index $dn_s/\ln k$ are small compared with the observed values $\mathcal{O}(-0.01)$. It might be interesting to consider whether we can improve this situation. One such possibility is to include a higher-dimensional operator [17]. In conclusion, the gauged $B-L$ extension of the SM is a phenomenologically very interesting model in that it can explain both the cosmological observations and electroweak symmetry breaking at $\mathcal{O}(100)$ GeV by breaking the MPP.

Acknowledgements

We thank Hikaru Kawai and Yuta Hamada for valuable discussions.

Funding

Open Access funding: SCOAP[3].

Appendix A. Two-loop renormalization group equations

The two-loop RGEs of the gauged $B-L$ model are as follows:[9]

$$\frac{d\Gamma_H}{dt}=\frac{1}{(4\pi)^2}\left(\frac{9}{4}g_2^2+\frac{3}{4}g_Y^2+\frac{3}{4}g_{\rm mix}^2-3y_t^2-3y_\nu^2\right), \tag{A1}$$

$$\frac{d\Gamma_\Psi}{dt}=\frac{1}{(4\pi)^2}\left(12g_{B-L}^2-\frac{3}{2}Y_R^2\right), \tag{A2}$$

$$\begin{aligned}\frac{dg_Y}{dt}=&\frac{1}{(4\pi)^2}\frac{41}{6}g_Y^3+\frac{g_Y^3}{(4\pi)^4}\left(\frac{199}{18}g_Y^2+\frac{9}{2}g_2^2+\frac{44}{3}g_3^2+\frac{92}{9}g_{B-L}^2+\frac{199}{18}g_{\rm mix}^2\right.\\&\left.+\frac{164}{9}g_{\rm mix}g_{B-L}-\frac{17}{6}y_t^2-\frac{3}{2}y_\nu^2\right),\end{aligned} \tag{A3}$$

[9] Our calculations are based on Refs. [37–40]. In particular, the two-loop results with an arbitrary number of Abelian groups are presented in Ref. [40].

$$\frac{dg_{\rm mix}}{dt} = \frac{1}{(4\pi)^2}\left(\frac{41}{6}g_{\rm mix}\left(g_{\rm mix}^2+2g_Y^2\right)+\frac{32}{3}g_{B-L}\left(g_{\rm mix}^2+g_Y^2\right)+12g_{\rm mix}g_{B-L}^2\right)$$
$$+\frac{1}{(4\pi)^4}\left\{g_{\rm mix}^3\left(\frac{199}{18}g_{\rm mix}^2+\frac{328}{9}g_{\rm mix}g_{B-L}+\frac{9}{2}g_2^2+\frac{44}{3}g_3^2+\frac{184}{3}g_{B-L}^2+\frac{199}{6}g_Y^2\right)\right.$$
$$+g_{\rm mix}^2\left(\frac{656}{9}g_Y^2g_{B-L}+\frac{448}{9}g_{B-L}^3+\frac{32}{3}g_3^2g_{B-L}+12g_2^2g_{B-L}\right)$$
$$+g_{\rm mix}\left(\frac{644}{9}g_Y^2g_{B-L}^2+\frac{800}{9}g_{B-L}^4+12g_2^2g_{B-L}^2+\frac{199}{9}g_Y^4+9g_2^2g_Y^2+\frac{88}{3}g_3^2g_Y^2+\frac{32}{3}g_3^2g_{B-L}^2\right)$$
$$+\frac{164}{9}g_Y^4g_{B-L}+\frac{224}{9}g_Y^2g_{B-L}^3+12g_2^2g_Y^2g_{B-L}+\frac{32}{3}g_3^2g_Y^2g_{B-L}$$
$$-y_t^2\left(\frac{10}{3}g_Y^2g_{B-L}+\frac{17}{6}g_{\rm mix}^3+\frac{10}{3}g_{\rm mix}^2g_{B-L}+\frac{4}{3}g_{\rm mix}g_{B-L}^2+\frac{17}{3}g_{\rm mix}g_Y^2\right)$$
$$\left.-y_\nu^2\left(6g_Y^2g_{B-L}+\frac{3}{2}g_{\rm mix}^3+3g_{\rm mix}g_Y^2+6g_{\rm mix}^2g_{B-L}+12g_{\rm mix}g_{B-L}^2\right)-3Y_R^2g_{\rm mix}g_{B-L}^2\right\}, \tag{A4}$$

$$\frac{dg_{B-L}}{dt} = \frac{g_{B-L}}{(4\pi)^2}\left(12g_{B-L}^2+\frac{32}{3}g_{B-L}g_{\rm mix}+\frac{41}{6}g_{\rm mix}^2\right)$$
$$+\frac{g_{B-L}}{(4\pi)^4}\left\{g_{B-L}^2\left(\frac{800}{9}g_{B-L}^2+\frac{92}{9}g_y^2+\frac{184}{3}g_{\rm mix}^2+12g_2^2+\frac{32}{3}g_3^2+\frac{448}{9}g_{\rm mix}g_{B-L}\right)\right.$$
$$+g_{B-L}\left(\frac{164}{9}g_{\rm mix}g_y^2+\frac{328}{9}g_{\rm mix}^3+12g_2^2g_{\rm mix}+\frac{32}{3}g_3^2g_{\rm mix}\right)$$
$$+\frac{199}{18}g_{\rm mix}^2g_y^2+\frac{199}{18}g_{\rm mix}^4+\frac{9}{2}g_2^2g_{\rm mix}^2+\frac{44}{3}g_3^2g_{\rm mix}^2$$
$$\left.-y_t^2\left(\frac{4}{3}g_{B-L}^2+\frac{10}{3}g_{\rm mix}g_{B-L}+\frac{17}{6}g_{\rm mix}^2\right)-y_\nu^2\left(6g_{\rm mix}g_{B-L}-\frac{3}{2}g_{\rm mix}^2-12g_{B-L}^2\right)-3Y_R^2g_{B-L}^2\right\}, \tag{A5}$$

$$\frac{dg_2}{dt} = -\frac{1}{(4\pi)^2}\frac{19}{6}g_2^3+\frac{g_2^3}{(4\pi)^4}\left(\frac{3}{2}g_Y^2+\frac{35}{6}g_2^2+12g_3^2+4g_{B-L}^2+\frac{3}{2}g_{\rm mix}^2+4g_{\rm mix}g_{B-L}-\frac{3}{2}y_t^2-\frac{3}{2}y_\nu^2\right), \tag{A6}$$

$$\frac{dg_3}{dt} = -\frac{7}{(4\pi)^2}g_3^3+\frac{g_3^3}{(4\pi)^4}\left(\frac{11}{6}g_Y^2+\frac{9}{2}g_2^2-26g_3^2+\frac{4}{3}g_{B-L}^2+\frac{11}{6}g_{\rm mix}^2+\frac{4}{3}g_{\rm mix}g_{B-L}-2y_t^2\right), \tag{A7}$$

$$\frac{dy_t}{dt} = \frac{y_t}{(4\pi)^2}\left(\frac{9}{2}y_t^2+3y_\nu^2-8g_3^2-\frac{9}{4}g_2^2-\frac{17}{12}g_Y^2-\frac{17}{12}g_{\rm mix}^2-\frac{2}{3}g_{B-L}^2-\frac{5}{3}g_{B-L}g_{\rm mix}\right)$$
$$+\frac{y_t}{(4\pi)^4}\left\{-12y_t^4-\frac{27}{4}y_\nu^4-\frac{27}{4}y_t^2y_\nu^2-\frac{9}{4}Y_R^2y_\nu^2+6\lambda^2+\frac{1}{2}\kappa^2-12\lambda y_t^2\right.$$
$$+y_t^2\left(36g_3^2+\frac{225}{16}g_2^2+\frac{131}{16}g_Y^2+3g_{B-L}^2+\frac{131}{16}g_{\rm mix}^2+\frac{25}{4}g_{\rm mix}g_{B-L}\right)$$
$$+y_\nu^2\left(\frac{45}{8}g_2^2+\frac{15}{8}g_Y^2+15g_{B-L}^2+\frac{15}{8}g_{\rm mix}^2+\frac{15}{2}g_{\rm mix}g_{B-L}\right)+\frac{502}{27}g_{\rm mix}^3g_{B-L}$$
$$+\frac{1085}{36}g_{\rm mix}^2g_{B-L}^2+\frac{502}{27}g_{\rm mix}g_Y^2g_{B-L}+\frac{665}{27}g_{\rm mix}g_{B-L}^3+\frac{9}{4}g_2^2g_{\rm mix}g_{B-L}-\frac{20}{9}g_3^2g_{\rm mix}g_{B-L}$$
$$+\frac{203}{27}g_{B-L}^4+\frac{3}{4}g_2^2g_{B-L}^2-\frac{8}{9}g_3^2g_{B-L}^2+\frac{91}{12}g_Y^2g_{B-L}^2+\frac{1187}{216}g_{\rm mix}^4-\frac{3}{4}g_2^2g_{\rm mix}^2$$
$$\left.+\frac{19}{9}g_3^2g_{\rm mix}^2+\frac{1187}{108}g_{\rm mix}^2g_Y^2-\frac{23}{4}g_2^4-108g_3^4+\frac{1187}{216}g_Y^4+9g_2^2g_3^2-\frac{3}{4}g_2^2g_Y^2+\frac{19}{9}g_3^2g_Y^2\right\}, \tag{A8}$$

$$\frac{dy_\nu}{dt} = \frac{y_\nu}{(4\pi)^2}\left(-3g_{\rm mix}g_{B-L} - 6g_{B-L}^2 - \frac{3}{4}g_{\rm mix}^2 - \frac{3}{4}g_Y^2 - \frac{9}{4}g_2^2 + \frac{1}{4}Y_R^2 + 3y_t^2 + \frac{9}{2}y_\nu^2\right)$$
$$+ \frac{y_\nu}{(4\pi)^4}\left\{-12y_\nu^4 - \frac{27}{4}y_t^4 - \frac{5}{4}Y_R^4 - y_\nu^2\left(\frac{27}{4}y_t^2 + \frac{21}{8}Y_R^2\right) + 6\lambda^2 + \frac{1}{2}\kappa^2 - 12\lambda y_\nu^2 - \kappa Y_R^2\right.$$
$$+ y_\nu^2\left(\frac{225}{16}g_2^2 + \frac{123}{16}g_Y^2 + 27g_{B-L}^2 + \frac{123}{16}g_{\rm mix}^2 + \frac{69}{4}g_{\rm mix}g_{B-L}\right)$$
$$+ y_t^2\left(20g_3^2 + \frac{45}{8}g_2^2 + \frac{85}{24}g_Y^2 + \frac{5}{3}g_{B-L}^2 + \frac{85}{24}g_{\rm mix}^2 + \frac{25}{6}g_{\rm mix}g_{B-L}\right)$$
$$+ Y_R^2\left(22g_{B-L}^2 + 3g_{\rm mix}g_{B-L}\right) + 21g_{\rm mix}^3g_{B-L} + \frac{799}{12}g_{\rm mix}^2g_{B-L}^2$$
$$+ 21g_{\rm mix}g_Y^2g_{B-L} + \frac{253}{3}g_{\rm mix}g_{B-L}^3 + \frac{9}{4}g_2^2g_{\rm mix}g_{B-L} + 65g_{B-L}^4 + \frac{27}{4}g_2^2g_{B-L}^2$$
$$\left. + \frac{187}{12}g_Y^2g_{B-L}^2 + \frac{35}{24}g_{\rm mix}^4 - \frac{9}{4}g_2^2g_{\rm mix}^2 + \frac{35}{12}g_{\rm mix}^2g_Y^2 - \frac{23}{4}g_2^4 + \frac{35}{24}g_Y^4 - \frac{9}{4}g_2^2g_Y^2\right\}, \tag{A9}$$

$$\frac{dY_R}{dt} = \frac{Y_R}{(4\pi)^2}\left(\frac{5}{2}Y_R^2 + 2y_\nu^2 - 6g_{B-L}^2\right)$$
$$+ \frac{Y_R}{(4\pi)^4}\left\{-5Y_R^4 - \frac{19}{2}Y_R^2y_\nu^2 - 9y_t^2y_\nu^2 - \frac{27}{2}y_\nu^4 + 4\lambda_\Psi^2 + \kappa^2 - 8\kappa y_\nu^2 - 8\lambda_\Psi Y_R^2\right.$$
$$+ y_\nu^2\left(\frac{51}{4}g_2^2 + \frac{17}{4}g_Y^2 + 16g_{B-L}^2 + \frac{17}{4}g_{\rm mix}^2 + 11g_{\rm mix}g_{B-L}\right) + \frac{103}{2}Y_R^2g_{B-L}^2$$
$$\left. - 127g_{B-L}^4 - \frac{35}{6}g_{\rm mix}^2g_{B-L}^2 - \frac{32}{3}g_{\rm mix}g_{B-L}^3\right\}, \tag{A10}$$

$$\frac{d\lambda_\Psi}{dt} = \frac{1}{(4\pi)^2}\left(\lambda_\Psi\left(20\lambda_\Psi - 48g_{B-L}^2 + 6Y_R^2\right) + 2\kappa^2 + 96g_{B-L}^4 - 3Y_R^4\right)$$
$$+ \frac{1}{(4\pi)^4}\left\{-240\lambda_\Psi^3 - 20\kappa^2\lambda_\Psi - 8\kappa^3 + \lambda_\Psi\left(\frac{1280}{3}g_{\rm mix}g_{B-L}^3 + \frac{844}{3}g_{\rm mix}^2g_{B-L}^2 + 2112g_{B-L}^4\right)\right.$$
$$+ 448\lambda_\Psi^2g_{B-L}^2 - 7168g_{B-L}^6 - \frac{8192}{3}g_{\rm mix}g_{B-L}^5 - \frac{5344}{3}g_{\rm mix}^2g_{B-L}^4$$
$$+ 12Y_R^4g_{B-L}^2 + 288Y_R^2g_{B-L}^4 + 30\lambda_\Psi Y_R^2g_{B-L}^2 - 60Y_R^2\lambda_\Psi^2 + \lambda_\Psi\left(3Y_R^4 - 18Y_R^2y_\nu^2\right)$$
$$\left. + 12Y_R^4y_\nu^2 + 12Y_R^6 - 12\kappa^2\left(y_t^2 + y_\nu^2\right) + \kappa^2\left(12g_2^2 + 4g_Y^2 + 4g_{\rm mix}^2\right) + 40\kappa g_{\rm mix}^2g_{B-L}^2\right\}, \tag{A11}$$

$$\frac{d\lambda}{dt} = \frac{1}{16\pi^2}\left(\lambda\left(24\lambda - 9g_2^2 - 3g_{\rm mix}^2 - 3g_Y^2 + 12y_t^2 + 12y_\nu^2\right) + \frac{3}{4}\left(g_Y^2 + g_{\rm mix}^2\right)g_2^2\right.$$
$$\left. + \frac{3}{4}g_{\rm mix}^2g_Y^2 + \frac{9}{8}g_2^4 + \frac{3}{8}g_{\rm mix}^4 + \frac{3}{8}g_Y^4 + \kappa^2 - 6y_t^4 - 6y_\nu^4\right)$$
$$+ \frac{1}{(4\pi)^4}\left\{-4\kappa^3 - 10\kappa^2\lambda - 312\lambda^3 + 36\lambda^2\left(g_Y^2 + g_{\rm mix}^2 + 3g_2^2\right)\right.$$
$$+ \lambda\left(\frac{629}{24}g_Y^4 + \frac{629}{24}g_{\rm mix}^4 + \frac{39}{4}g_{\rm mix}^2g_2^2 + \frac{39}{4}g_Y^2g_2^2 - \frac{73}{8}g_2^4 + \frac{80}{3}g_{B-L}g_{\rm mix}^3 + 34g_{B-L}^2g_{\rm mix}^2\right.$$
$$\left. + \frac{629}{12}g_{\rm mix}^2g_Y^2 + \frac{80}{3}g_{B-L}g_{\rm mix}g_Y^2\right) + \frac{305}{16}g_2^6 - \frac{289}{48}g_{\rm mix}^2g_2^4 - \frac{289}{48}g_Y^2g_2^4$$
$$- \frac{559}{48}g_{\rm mix}^4g_2^2 - \frac{559}{48}g_Y^4g_2^2 - \frac{32}{3}g_{B-L}g_{\rm mix}^3g_2^2 - 13g_{B-L}^2g_{\rm mix}^4 - \frac{379}{16}g_{\rm mix}^2g_Y^4 - \frac{32}{3}g_{B-L}g_{\rm mix}g_Y^4$$

$$
\begin{aligned}
&- \frac{32}{3} g_{B-L} g_{\rm mix}^5 - 13 g_{B-L}^2 g_{\rm mix}^2 g_2^2 - \frac{559}{24} g_{\rm mix}^2 g_Y^2 g_2^2 - \frac{379}{48} g_{\rm mix}^6 - \frac{379}{48} g_Y^6 \\
&- \frac{32}{3} g_{B-L} g_{\rm mix} g_Y^2 g_2^2 - \frac{379}{16} g_{\rm mix}^4 g_Y^2 - \frac{64}{3} g_{B-L} g_{\rm mix}^3 g_Y^2 - 13 g_{B-L}^2 g_{\rm mix}^2 g_Y^2 \\
&- y_t^4 \left(\frac{8}{3} g_Y^2 + 32 g_3^2 + \frac{8}{3} g_{B-L}^2 + \frac{8}{3} g_{\rm mix}^2 + \frac{20}{3} g_{B-L} g_{\rm mix} \right) - y_\nu^4 \left(24 g_{B-L}^2 + 12 g_{B-L} g_{\rm mix} \right) \\
&+ y_t^2 \left(\frac{21}{2} g_{\rm mix}^2 g_2^2 + \frac{21}{2} g_Y^2 g_2^2 + 6 g_{B-L} g_{\rm mix} g_2^2 - \frac{9}{4} g_2^4 - \frac{19}{4} g_{\rm mix}^4 \right. \\
&\left. - \frac{19}{4} g_Y^4 - \frac{19}{2} g_{\rm mix}^2 g_Y^2 - 4 g_{B-L}^2 g_{\rm mix}^2 - 10 g_{B-L} g_{\rm mix}^3 - 10 g_{B-L} g_{\rm mix} g_Y^2 \right) \\
&- y_\nu^2 \left(\frac{3}{2} g_{\rm mix}^2 g_2^2 + \frac{3}{2} g_Y^2 g_2^2 + 18 g_{B-L} g_{\rm mix} g_2^2 + \frac{9}{4} g_2^4 + \frac{3}{4} g_{\rm mix}^4 + \frac{3}{4} g_Y^4 + 18 g_{B-L} g_{\rm mix}^3 \right. \\
&\left. + 36 g_{B-L}^2 g_{\rm mix}^2 + \frac{3}{2} g_{\rm mix}^2 g_Y^2 + 18 g_{B-L} g_{\rm mix} g_Y^2 \right) + \lambda y_t^2 \left(\frac{45}{2} g_2^2 + 80 g_3^2 + \frac{85}{6} g_Y^2 + \frac{85}{6} g_{\rm mix}^2 \right. \\
&\left. + \frac{20}{3} g_{B-L}^2 + \frac{50}{3} g_{B-L} g_{\rm mix} \right) + \lambda y_\nu^2 \left(\frac{45}{2} g_2^2 + \frac{15}{2} g_Y^2 + 60 g_{B-L}^2 + \frac{15}{2} g_{\rm mix}^2 + 30 g_{B-L} g_{\rm mix} \right) \\
&- 144 \lambda^2 \left(y_t^2 + y_\nu^2 \right) - 3\lambda \left(y_t^4 + y_\nu^4 + 3 y_\nu^2 Y_R^2 \right) + 30 y_t^6 + 30 y_\nu^6 + 12 y_\nu^4 Y_R^2 - 3\kappa^2 Y_R^2 \\
&+ 32 \kappa^2 g_{B-L}^2 + 20 \kappa g_{B-L}^2 g_{\rm mix}^2 \Big\}, \qquad \text{(A12)}
\end{aligned}
$$

$$
\begin{aligned}
\frac{d\kappa}{dt} = &\frac{1}{(4\pi)^2} \left\{ \kappa \left(4\kappa + 12\lambda + 8\lambda_\Psi - \frac{3}{2} g_y^2 - 24 g_{B-L}^2 - \frac{3}{2} g_{\rm mix}^2 \right. \right. \\
&\left. \left. - \frac{9}{2} g_2^2 + 3 Y_R^2 + 6 y_t^2 + 6 y_\nu^2 \right) + 12 g_{\rm mix}^2 g_{B-L}^2 - 12 Y_R^2 y_\nu^2 \right\} \\
&+ \frac{1}{(4\pi)^4} \left\{ \kappa \left(-11\kappa^2 - 40\lambda_\Psi^2 - 48\kappa\lambda_\Psi - 60\lambda^2 - 72\kappa\lambda \right. \right. \\
&\left. \left. - \left(y_t^2 + y_\nu^2 \right) (12\kappa + 72\lambda) - Y_R^2 (6\kappa + 24\lambda_\Psi) - \frac{27}{2} y_t^4 - \frac{27}{2} y_\nu^4 \right. \right. \\
&\left. \left. - \frac{9}{2} Y_R^4 + \frac{21}{2} y_\nu^2 Y_R^2 + g_2^2 (3\kappa + 72\lambda) + g_Y^2 (\kappa + 24\lambda) + g_{B-L}^2 (16\kappa + 256\lambda_\Psi) \right. \right. \\
&\left. \left. + g_{\rm mix}^2 (\kappa + 24\lambda) + y_t^2 \left(\frac{45}{4} g_2^2 + 40 g_3^2 + \frac{10}{3} g_{B-L}^2 + \frac{85}{12} g_{\rm mix}^2 + \frac{85}{12} g_Y^2 + \frac{25}{3} g_{B-L} g_{\rm mix} \right) \right. \right. \\
&\left. \left. + y_\nu^2 \left(\frac{45}{4} g_2^2 + 30 g_{B-L}^2 + \frac{15}{4} g_{\rm mix}^2 + \frac{15}{4} g_Y^2 + 15 g_{B-L} g_{\rm mix} \right) + 15 Y_R^2 g_{B-L}^2 \right. \right. \\
&\left. \left. - \frac{145}{16} g_2^4 + \frac{557}{48} g_Y^4 + 672 g_{B-L}^4 + \frac{557}{48} g_{\rm mix}^4 + \frac{15}{8} g_{\rm mix}^2 g_2^2 + \frac{15}{8} g_Y^2 g_2^2 + \frac{40}{3} g_{B-L} g_{\rm mix}^3 \right. \right. \\
&\left. \left. + \frac{497}{3} g_{B-L}^2 g_{\rm mix}^2 + \frac{557}{24} g_{\rm mix}^2 g_Y^2 + \frac{40}{3} g_{B-L} g_{\rm mix} g_Y^2 + \frac{640}{3} g_{B-L}^3 g_{\rm mix} \right) \right. \\
&\left. + y_\nu^2 Y_R^2 \left(30 Y_R^2 + 66 y_\nu^2 - 84 g_{B-L}^2 - \frac{3}{2} g_{\rm mix}^2 - \frac{3}{2} g_Y^2 - 24 g_{B-L} g_{\rm mix} + \frac{9}{2} g_2^2 \right) \right. \\
&\left. - y_t^2 \left(64 g_{B-L}^4 + 76 g_{B-L}^2 g_{\rm mix}^2 + 160 g_{B-L}^3 g_{\rm mix} \right) - y_\nu^2 \left(576 g_{B-L}^4 + 12 g_{B-L}^2 g_{\rm mix}^2 + 288 g_{B-L}^3 g_{\rm mix} \right) \right. \\
&\left. - 18 g_{B-L}^2 g_{\rm mix}^2 Y_R^2 + 80 \lambda_\Psi g_{B-L}^2 g_{\rm mix}^2 + 120 \lambda g_{B-L}^2 g_{\rm mix}^2 - 45 g_{B-L}^2 g_{\rm mix}^2 g_2^2 - \frac{713}{3} g_{B-L}^2 g_{\rm mix}^4 \right. \\
&\left. - \frac{1024}{3} g_{B-L}^3 g_{\rm mix}^3 - 656 g_{B-L}^4 g_{\rm mix}^2 - \frac{713}{3} g_{B-L}^2 g_{\rm mix}^2 g_Y^2 - \frac{512}{3} g_{B-L}^3 g_{\rm mix} g_Y^2 \right\}. \qquad \text{(A13)}
\end{aligned}
$$

References

[1] G. Aad et al. [ATLAS Collaboration], Phys. Lett. B **716**, 1 (2012) [arXiv:1207.7214 [hep-ex]] [Search INSPIRE].
[2] S. Chatrchyan et al. [CMS Collaboration], Phys. Lett. B **716**, 30 (2012) [arXiv:1207.7235 [hep-ex]] [Search INSPIRE].
[3] C. D. Froggatt and H. B. Nielsen, Phys. Lett. B **368**, 96 (1996) [arXiv:hep-ph/9511371] [Search INSPIRE].
[4] C. D. Froggatt, H. B. Nielsen, and Y. Takanishi, Phys. Rev. D **64**, 113014 (2001) [arXiv:hep-ph/0104161] [Search INSPIRE].
[5] H. B. Nielsen, [arXiv:1212.5716 [hep-ph]] [Search INSPIRE].
[6] D. Buttazzo, G. Degrassi, P. P. Giardino, G. F. Giudice, F. Sala, A. Salvio, and A. Strumia, J. High Energy Phys. **1312**, 089 (2013) [arXiv:1307.3536 [hep-ph]] [Search INSPIRE].
[7] M. Shaposhnikov and C. Wetterich, Phys. Lett. B **683**, 196 (2010) [arXiv:0912.0208 [hep-th]] [Search INSPIRE].
[8] K. A. Meissner and H. Nicolai, Phys. Lett. B **660**, 260 (2008) [arXiv:0710.2840 [hep-th]] [Search INSPIRE].
[9] V. V. Khoze, C. McCabe, and G. Ro, J. High Energy Phys. **1408**, 026 (2014) [arXiv:1403.4953 [hep-ph]] [Search INSPIRE].
[10] H. Kawai and T. Okada, Prog. Theor. Phys. **127**, 689 (2012) [arXiv:1110.2303 [hep-th]] [Search INSPIRE].
[11] H. Kawai, Int. J. Mod. Phys. A **28**, 1340001 (2013)
[12] Y. Hamada, H. Kawai, and K. Kawana, Int. J. Mod. Phys. A **29**, 1450099 (2014) [arXiv:1405.1310 [hep-ph]] [Search INSPIRE].
[13] Y. Hamada, H. Kawai, and K. Kawana, [arXiv:1409.6508 [hep-ph]] [Search INSPIRE].
[14] F. L. Bezrukov and M. Shaposhnikov, Phys. Lett. B **659**, 703 (2008) [arXiv:0710.3755 [hep-th]] [Search INSPIRE].
[15] Y. Hamada, H. Kawai, and K. y. Oda, Prog. Theor. Exp. Phys. **2014**, 023B02 (2014) [arXiv:1308.6651 [hep-ph]] [Search INSPIRE].
[16] Y. Hamada, H. Kawai, K. y. Oda, and S. C. Park, Phys. Rev. Lett. **112**, 241301 (2014) [arXiv:1403.5043 [hep-ph]] [Search INSPIRE].
[17] Y. Hamada, H. Kawai, K. y. Oda, and S. C. Park, Phys. Rev. D **91**, 053008 (2015) [arXiv:1408.4864 [hep-ph]] [Search INSPIRE].
[18] Y. Hamada, K. y. Oda, and F. Takahashi, Phys. Rev. D **90**, 097301 (2014) [arXiv:1408.5556 [hep-ph]] [Search INSPIRE].
[19] Y. Kawamura, Prog. Theor. Exp. Phys. **2013**, 113B04 (2013) [arXiv:1308.5069 [hep-ph]] [Search INSPIRE].
[20] K. A. Meissner and H. Nicolai, Phys. Lett. B **648**, 312 (2007) [arXiv:hep-th/0612165] [Search INSPIRE].
[21] N. Haba, H. Ishida, K. Kaneta, and R. Takahashi, Phys. Rev. D **90**, 036006 (2014) [arXiv:1406.0158 [hep-ph]] [Search INSPIRE].
[22] Y. Hamada, H. Kawai, and K. y. Oda, [arXiv:1501.04455 [hep-ph]] [Search INSPIRE].
[23] Y. Hamada, H. Kawai, and K. y. Oda, J. High Energy Phys. **1407**, 026 (2014) [arXiv:1404.6141 [hep-ph]] [Search INSPIRE].
[24] K. Kawana, [arXiv:1411.2097 [hep-ph]] [Search INSPIRE].
[25] S. Iso, N. Okada, and Y. Orikasa, Phys. Lett. B **676**, 81 (2009) [arXiv:0902.4050 [hep-ph]] [Search INSPIRE].
[26] S. Iso and Y. Orikasa, Prog. Theor. Exp. Phys. **2013**, 023B08 (2013) [arXiv:1210.2848 [hep-ph]] [Search INSPIRE].
[27] N. Okada and O. Seto, Phys. Rev. D **82**, 023507 (2010) [arXiv:1002.2525 [hep-ph]] [Search INSPIRE].
[28] N. Okada, M. U. Rehman, and Q. Shafi, Phys. Lett. B **701**, 520 (2011) [arXiv:1102.4747 [hep-ph]] [Search INSPIRE].
[29] G. Aad et al. [ATLAS Collaboration], Phys. Rev. D **90**, 052005 (2014) [arXiv:1405.4123 [hep-ex]] [Search INSPIRE].
[30] P. H. Chankowski, S. Pokorski, and J. Wagner, Eur. Phys. J. C **47**, 187 (2006) [arXiv:hep-ph/0601097] [Search INSPIRE].

[31] M. S. Carena, A. Daleo, B. A. Dobrescu, and T. M. P. Tait, Phys. Rev. D **70**, 093009 (2004) [arXiv:hep-ph/0408098] [Search INSPIRE].
[32] P. A. R. Ade et al. [Planck Collaboration], [arXiv:1502.01589 [astro-ph.CO]] [Search INSPIRE].
[33] P. A. R. Ade et al. [BICEP2 Collaboration], Phys. Rev. Lett. **112**, 241101 (2014) [arXiv:1403.3985 [astro-ph.CO]] [Search INSPIRE].
[34] M. J. Mortonson and U. Seljak, J. Cosmol. Astropart. Phys. **1410**, 035 (2014) [arXiv:1405.5857 [astro-ph.CO]] [Search INSPIRE].
[35] R. Flauger, J. C. Hill, and D. N. Spergel, J. Cosmol. Astropart. Phys. **1408**, 039 (2014) [arXiv:1405.7351 [astro-ph.CO]] [Search INSPIRE].
[36] N. Okada, V. N. Şenoğuz, and Q. Shafi, [arXiv:1403.6403 [hep-ph]] [Search INSPIRE].
[37] M. E. Machacek and M. T. Vaughn, Nucl. Phys. B **222**, 83 (1983).
[38] M. E. Machacek and M. T. Vaughn, Nucl. Phys. B **236**, 221 (1984).
[39] M. E. Machacek and M. T. Vaughn, Nucl. Phys. B **249**, 70 (1985).
[40] R. M. Fonseca, M. Malinský, and F. Staub, Phys. Lett. B **726**, 882 (2013). [arXiv:1308.1674 [hep-ph]] [Search INSPIRE].